Order-disorder behavior in KNbO₃ and KNbO₃/KTaO₃ solid solutions and superlattices by molecular-dynamics simulation

S. R. PHILLPOT
*Department of Materials Science and Engineering, University of Florida,
Gainesville FL 32611, USA*
E-mail: sphil@mse.ufl.edu

M. SEPLIARSKY, M. G. STACHIOTTI, R. L. MIGONI
Instituto de Fisica Rosario, CONICET-UNR, Rosario, Argentina

S. K. STREIFFER
Materials Science Division, Argonne National Laboratory, Argonne IL 60439, USA

We use molecular-dynamics simulation to examine the order-disorder behavior in pure ferroelectric KNbO₃and in KNbO₃-KTaO₃ ferroelectric-paraelectric solid solutions and superlattices. We find that the order-disorder behavior is remarkably robust and plays an important role in both the polarization rotation associated with switching of the perfect crystal and in the dynamical behavior of the solid solutions and superlattices.
© *2005 Springer Science + Business Media, Inc.*

1. Introduction

Potassium niobate (KNbO₃) is a perovskite ferroelectric, displaying transitions from the paraelectric cubic to ferroelectric tetragonal, orthorhombic and rhombohedral phases with decreasing temperature. It is well-known that KNbO₃ displays order-disorder behavior, characterized by the Nb and O ions hardly ever being at their crystallographically assigned positions even in the cubic phase. As a consequence, even in the cubic phase every unit cell is polarized at almost every instant of time: only the time-average macroscopic polarization is actually zero.

In this paper, we illustrate how this order-disorder behavior is manifested in a number of different scenarios. In each case, KNbO₃ is in an environment very far from that which it usually experiences in an equilibrium perfect crystal. In particular, we examine the dynamical behavior associated with polarization rotation during the switching of a perfect crystal and the coupling of order-disorder behavior with the displacive dynamics of paraelectric KTaO₃ in solid solutions and superlattices.

2. Polarization rotation in a perfect crystal

We have previously developed and validated an atomic-level simulation method for KNbO₃ based on a traditional shell-model description [1] of the ionic interactions in the system [2]; we use this interatomic description here. Our model of KNbO₃ displays the order-disorder type behavior seen experimentally [3]. This is illustrated by Fig. 1, which shows the distribution of the Cartesian components of polarization in a KNbO₃ perfect crystal in the cubic phase and in the orthorhombic phase. In the cubic phase the distribution functions for all three components of polarization are essentially identical, each showing a double-peaked structure with peaks at $\pm 30\ \mu$C/cm^2 and a minimum at $P = 0$; this is order-disorder behavior. Similar order-disorder behavior is seen in the tetragonal phase. In the orthorhombic phase by contrast, the system is polarized along the [011] direction, as characterized by the large components of polarization in the y-z plane. The polarization in the x-direction is zero on average; however, the distribution function consists of an extremely broad single peak. While such a unimodal distribution is characteristic of displacive behavior, the extremely broad flat top is atypical and suggests an admix of order-disorder behavior also. It has been seen experimentally that the orthorhombic phase, indeed, has a more displacive character [4].

To address the question of how this order-disorder behavior plays out in the switching behavior, we have simulated polarization switching in a surface-free, single-domain material [5]. We simulated a 3-d periodically repeated perfect crystal in the tetragonal phase with the initial polarization parallel to the [001] direction, i.e., $P_z > 0$. In the tetragonal phase, the polarization of any unit cell at any time is equally likely to be directed along any one of four equivalent crystallographic directions: [111], [$\bar{1}$11], [1$\bar{1}$1] and [$\bar{1}\bar{1}$1]. To force the polarization reversal, an external electric field, $E_z = 5 \times 10^5$ V/cm, was applied along the [00$\bar{1}$] direction; we found that this electric field is large enough to reverse the polarization, while an electric field of 10^5 V/cm cannot reverse the polarization on molecular-dynamics time
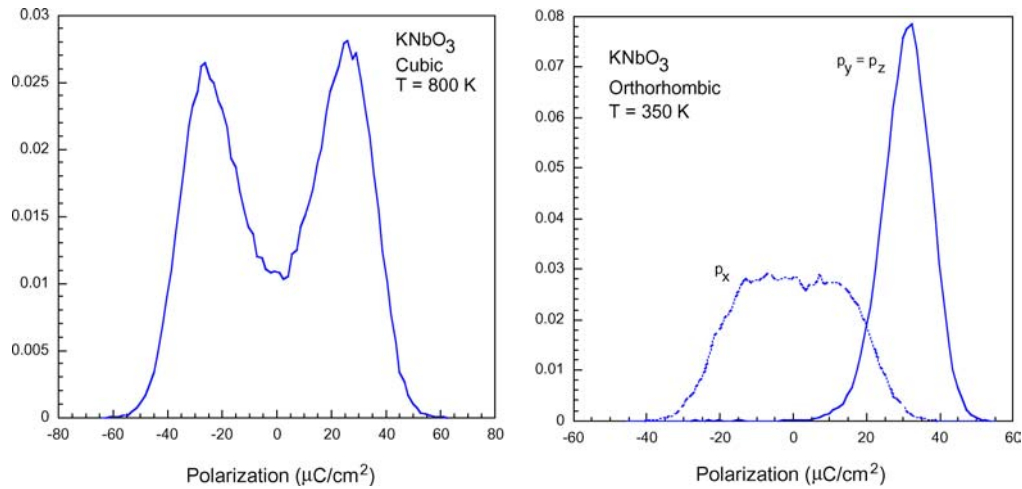
Figure 1 Distribution functions for the component of polarization in the cubic phase (left) and the orthorhombic phase of $KNbO_3$ (right) exemplify order-disorder and displacive dynamics respectively.
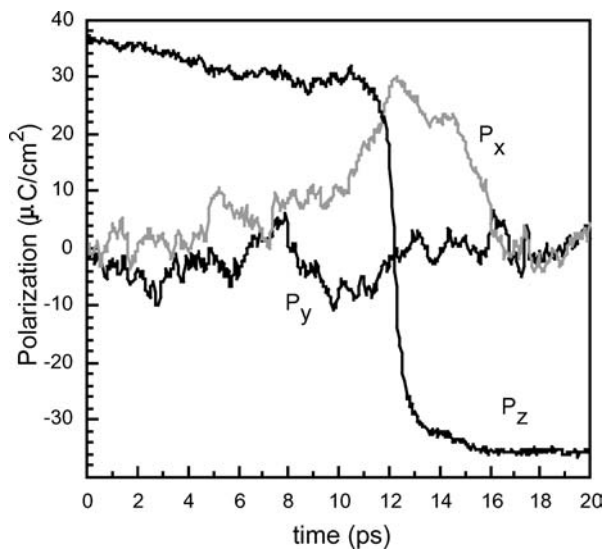

Figure 2 Time evolution of the three components of polarization through the reversal of P_z at $|E| = 5 \times 10^5$ V/cm and $T = 600$ K. Note that while P_y remains essentially zero throughout, the transition involves a significant increase and subsequent decrease in P_x.

scales. In order to allow full coupling between strain and polarization, all of our simulations were performed at zero pressure by the imposition of a Parinello-Rahman constant-pressure scheme [6].

We first consider the low-E ($E_z = 5 \times 10^5$ V/cm), low-T ($T = 600$ K) regime. Fig. 2 shows that P_z switches from $+36 \, \mu C/cm^2$ to $-36 \, \mu C/cm^2$ over a time interval of ~ 4 psecs. Throughout the switching process, P_y remains close to zero. However, P_x changes significantly through the switching process, resulting in $P \parallel$ to [011] at $t \sim 11.5$ ps, $\parallel$ to [010] at $t \sim 12$ ps and, $\parallel$ to [01$\bar{1}$] at $t \sim 13$ ps. (Presumably, the selection of [011] over the three other crystallographically equivalent orientations is purely stochastic.) That this can be considered as a rotation of the polarization, is confirmed by the observation that the magnitude of the total polarization is essentially constant throughout the switching process. The time evolution of the lattice parameters and the crystallographic angles are entirely consistent with this evolution of the polarization, confirming that the

polarization reverses through intermediate orthorhombic, tetragonal and orthorhombic states.

We have also performed a more detailed characterization of the polarization reversal process in terms of the order-disorder behavior [5]. To do this it is convenient to think in terms of the eight-site model of order-disorder behavior (see inset to Fig. 3) [3, 7]. Fig. 3 shows the
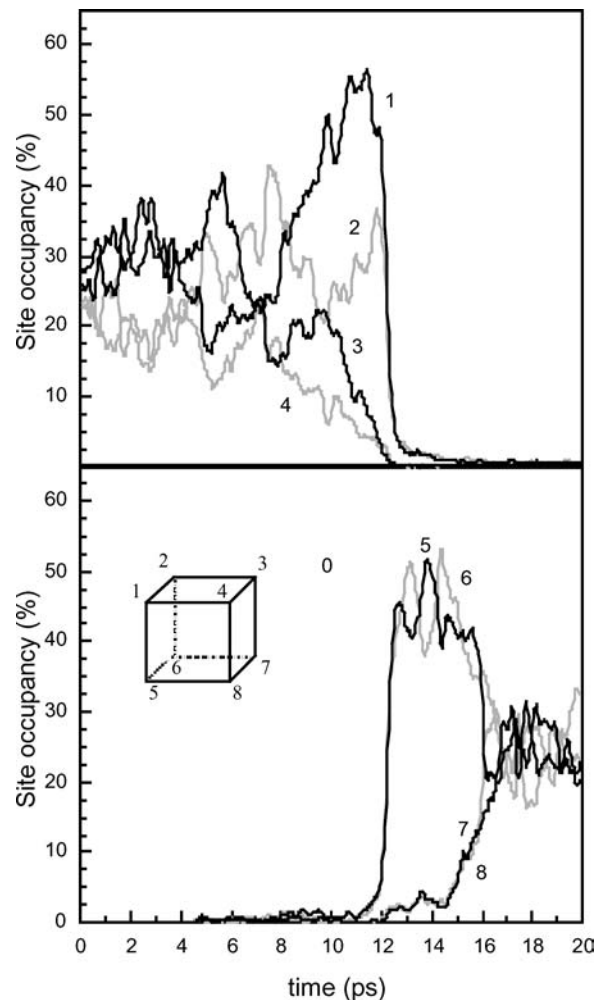

Figure 3 Time evolution of the probability of occupancy of each of the eight sites (inset) associated with the order-disorder transition in Fig. 2.

time evolution of the occupancy of these eight sites in a single unit cell. For early times sites 1, 2, 3 and 4 are each visited ~25% of the time in each unit cell, while sites 5, 6, 7 and 8 are unvisited; this is characteristic of an [001] polarized system. By about $t \sim 10$ ps, sites 3 and 4 are becoming less frequently visited, while sites 1 and 2 are more frequently visited (though not quite with equal probability); this is consistent with the orthorhombic phase seen in Figs 1 and 2. By $t \sim 12$ ps sites 1, 2, 5 and 6 are now equally often visited, characteristic of a tetragonal state with polarization parallel to [010]; this state is an extremely short-lived transient however.

After again passing through an orthorhombic phase involving sites 5 and 6, which has a lifetime of ~4 ps, the system finally settles into the tetragonal state with the polarization reversed and equal occupancy of sites 5, 6, 7 and 8. We have analyzed the spatial propagation in the system and find that while chains of reversed polarization tend to form parallel to the applied electric field, the component of polarization normal to the applied field is essentially spatially uncorrelated.

When the temperature is raised from 600 K to 675 K the evolution of the system changes in a qualitative manner. Although, microscopically, each unit cell evolves in essentially the manner described above, macroscopically the reversal of P_z is very rapid with no clear intermediate states. Moreover we find that P_x and P_y remain essentially zero throughout the switching process, characteristic of the switching of a set of essentially decoupled unit cells. As a result of this uncorrelated switching in the polarization, the transient intermediate state is approximately cubic, as illustrated in Fig. 4. Consistent with this, analysis in terms of the eight-site model shows an abrupt transition from sites 1, 2, 3 and 4 being occupied to states 5, 6, 7 and 8 being occupied.

It is interesting that this dynamic non-equilibrium process appears to follow the static energy surface. We recall that with increasing temperature $KNbO_3$ is stable in the rhombohedral, orthorhombic, tetragonal and cubic phases: it is thus natural that the tetragonal phase reorients via an intermediate orthorhombic rather than rhombohedral state.

A rather similar polarization rotation process has recently been seen experimentally during switching of $PbZn_{1/3}Nb_{2/3}O_3$–$PbTiO_3$ relaxors [8]. The mechanism of polarization rotation has also been proposed as underlying the large piezoelectric response in relaxors [9, 10] and has recently been experimentally confirmed [11].

3. Order-disorder behavior in solid solutions and superlattices

The above discussion demonstrates the rather robust nature of the order-disorder behavior in $KNbO_3$. We now turn to the issue of its stability in environments in which it is in intimate contact with a material with rather different dynamics. In particular, $KTaO_3$ has the same crystal structure as $KNbO_3$ but, as an incipient ferroelectric, is cubic at all temperatures. $KNbO_3$ and $KTaO_3$ are mutually soluble and form coherent superlattice structures. We have simulated both the $KTa_{0.5}Nb_{0.5}O_3$ (KTN) solid solution and <001>-oriented $KNbO_3/KTaO_3$ superlattices.

To dissect the ferroelectric response of KTN, it is useful to examine the distribution in the polarizations of the Ta-containing and Nb-containing unit cells. Fig. 5 shows the polarization distribution functions of the Nb-cells and Ta-cells in the tetragonal phase of KTN. We see that P_z for both Ta- and Nb-containing unit cells is narrowly peaked at a finite value, showing a significant polarization in this direction The double-peak structure in P_x and P_y for the Nb-containing cells is characteristic of order-disorder behavior. By contrast, the polarization distribution in the Ta-containing cells is broadened and shows hints of a double-peak structure; this is characteristic of largely displacive behavior with, perhaps, a small admixture of order-disorder.
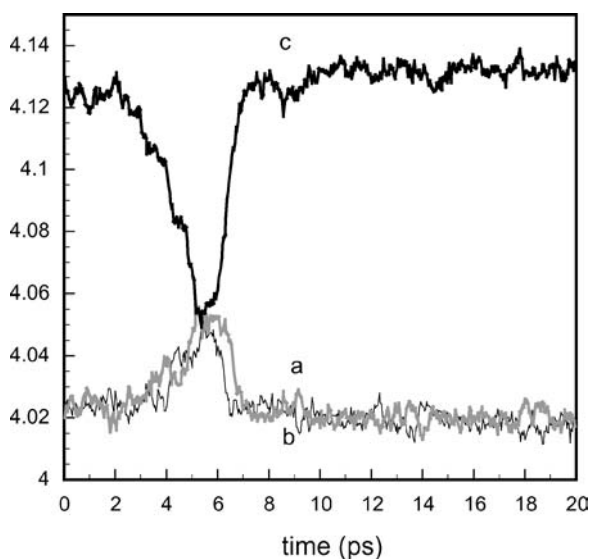

Figure 4 Time evolution of the three Cartesian lattice parameters during the polarization reversal at $T = 675$ K under an applied electric field of $|E| = 5 \times 10^5$ V/cm.
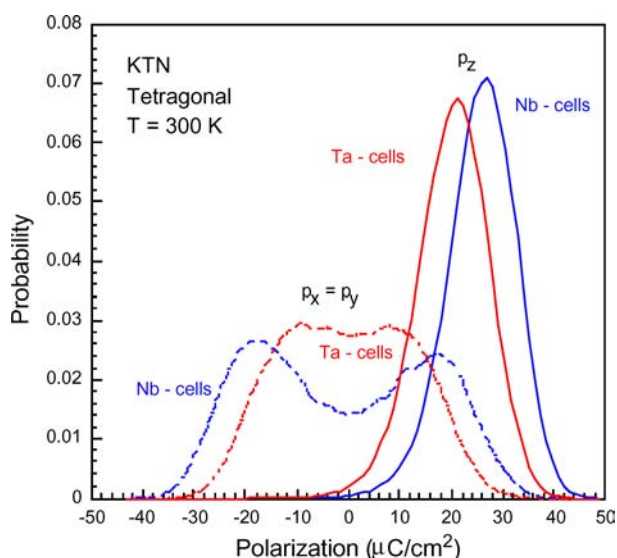

Figure 5 Polarization distribution functions in Nb-containing and Ta-containing unit cells in the tetragonal phase.

We have simulated both the zero-temperature [12, 13] and finite-temperature [14] structure and properties of $KNbO_3/KTaO_3$ superlattices on a $KTaO_3$ substrate. All of our simulations used a three-dimensionally periodic simulation cell and thus did not explicitly simulate the substrate or the free surface at the top of the superlattice. However, the effects of the substrate were incorporated by fixing the in-plane lattice parameters to those of perfect-crystal $KTaO_3$ at the same temperature, determined from independent simulations. The simulation cell consists of four alternating equal-thickness layers of $KNbO_3$ and $KTaO_3$. The modulation length, Λ, is the thickness of a $KNbO_3/KTaO_3$ bilayer in lattice parameters.

To explore the dynamical behavior in the superlattices, we determined the distribution functions for the component of polarization in the $KNbO_3$ and $KTaO_3$ layers in the modulation direction. Fig. 6 shows the polarization distribution functions separately for the $KNbO_3$ and $KTaO_3$ layers both above and below the Curie temperature, T_c, for $\Lambda = 6$ (representative of the regime in which $KNbO_3$ layers are strongly coupled through intermediate $KTaO_3$ layers) and $\Lambda = 18$ (representative of weaker coupling of $KNbO_3$ layers). Considering $\Lambda = 6$ first: below T_c the distribution functions for Nb-containing (solid line) and Ta-containing (dotted line) unit cells are very similar, reflecting only a very weak spatial dependence of P_z through the superlattices. However, the polarization distribution functions

for $KNbO_3$ and $KTaO_3$ above T_c are rather different from each other. Although both are extremely broad and approximately symmetric about $P_z = 0$, reflecting a net zero polarization, the distributions for the KTO layer is peaked at $P_z = 0$ reflecting essentially displacive behavior while the distribution function for the $KNbO_3$ is flatter with the indication of weak peaks at $P_z = \pm 20 \ \mu C/cm^2$; this is consistent with weak order-disorder type behavior.

It is instructive to compare these distribution functions to those for $\Lambda = 18$. At $T = 300$ K, just below the T_c, the coupling between $KNbO_3$ layers is much weaker than for $\Lambda = 6$, reflected by the significant difference in the average polarizations. That the $KTaO_3$ layer is much more weakly polarized than the $KNbO_3$ layer indicates that the behavior of the individual layers is more bulk-like than for $\Lambda = 6$. The order-disorder behavior in the $KNbO_3$ layers above T_c is clearly evident in the very strong double-peak structure centered at $P_z = \pm 30 \ \mu C/cm^2$. Moreover, the displacive nature in the $KTaO_3$ is evident from the presence of a single peak centered around $P_z = 0$. That the distribution function for the $KTaO_3$ at 450 K for $\Lambda = 18$ is actually more strongly peaked than that for $\Lambda = 6$ at 350 K while that of the $KNbO_3$ is more bimodal, is indicative of the much weaker coupling between the layers at larger Λ.

4. Concluding remarks

By looking at $KNbO_3$ in a variety of environments, we have seen that the order-disorder behavior is fundamental to its dynamical behavior. Perhaps this should not be surprising since the energy surface that produces the complex phase behavior of $KNbO_3$ is also intimately involved in the dynamical behavior. In particular, we saw that in the order-disorder system, the magnitude of the polarization is approximately constant during switching; i.e., the polarization essentially rotates in a discontinuous manner from one state to the next. Since $BaTiO_3$ has the same sequence of phase transitions and is also an order-disorder system, it can be expected to have rather similar dynamical behavior.
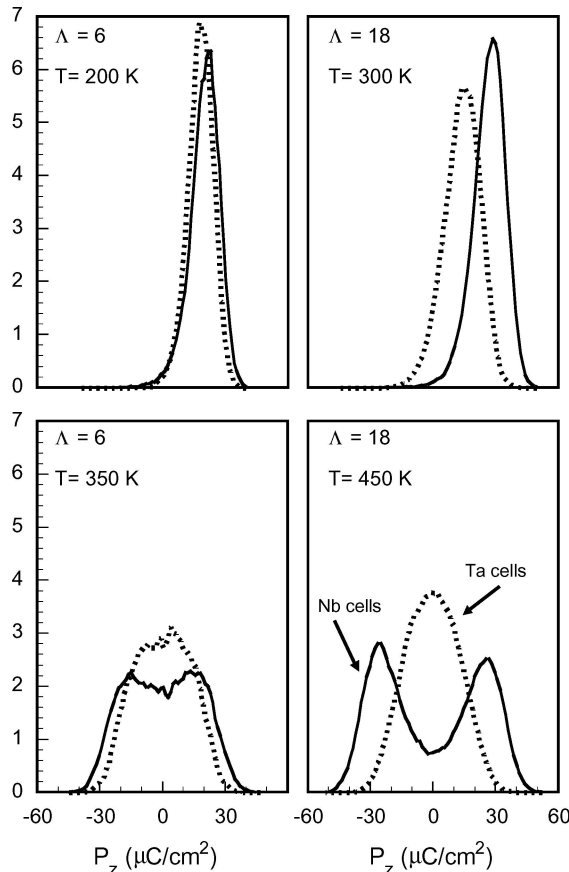

Figure 6 Polarization distribution functions for P_z in the $KNbO_3$ (solid line) and $KTaO_3$ (dashed line) layers for two different modulation lengths and two different temperatures. Left panels: $\Lambda = 6$, $T = 200$ K and $T = 250$ K, right panels: $\Lambda = 18$, $T = 300$ K and $T = 450$ K.

References

1. B. G. DICK and A. W. OVERHAUSER, *Phys. Rev.* **112** (1958) 90.
2. M. SEPLIARSKY, S. R. PHILLPOT, D. WOLF, M. G. STACHIOTTI and R. L. MIGONI, *Appl. Phys. Lett.* **76** (2000) 3986.
3. R. COMES, M. LAMBERT and A. GUINIER, *Sol. Stat. Comm.* **6** (1968) 715.
4. M. D. FONTANA, A. RIDAH, G. E. KUGEL and C. CARABATOS-NEDELEC, *J. Phys. C: Solid State Phys.* **21** (1988) 5853.
5. M. SEPLIARSKY, S. R. PHILLPOT, S. K. STREIFFER, M. G. STACHIOTTI and R. L. MIGONI, *Appl. Phys. Lett.* **79** (2001) 4417.
6. M. PARRINELLO and A. RAHMAN, *J. Appl. Phys.* **52** (1981) 7182.
7. R. Comes, M. Lambert and A. GUINIER, *Acta Cryst.* **18** (1970) 441.
8. J. YIN and W. CAO, *Appl. Phys. Lett.* **79** (2001) 4556.

9. A. GARCIA and D. VANDERBILT, *ibid.* **72** (1998) 2981.
10. H. FU and R. E. COHEN, *Nature* **403** (2000) 281.
11. B. NOHEDA, D. E. COX, G. SHIRANE, S.-E. PARK, L. E. CROSS and Z. ZHONG, *Phys. Rev. Lett.* **86** (2001) 3891.
12. M. SEPLIARSKY, S. R. PHILLPOT, D. WOLF, M. G. STACHIOTTI and R. L.MIGONI, *Phys. Rev. B* **64** (2001) 010601(R).
13. *Idem.*, *J. Appl. Phys.* **90** (2001) 4509.
14. M. SEPLIARSKY, S. R. PHILLPOT, M. G. STACHIOTTI and R. L. MIGONI, *ibid.* **91** (2002) 3165.